

A Numerical Study Using a Two-Dimensional Finite Elements Method to Analyze the Stability of Seven Tunnel Transversal Sections

GUÉMIDI Ismahene^{*1,2}, TALEB Hosni Abderrahmane^{1,3}, ELBAHI Bachir,^{4,5} AHMED Mustafa kamel Mohamed

¹FIMAS Laboratory, University of Bechar – ALGERIA.

²University Chadli Bendjedid of El Tarf, ALGERIA.

³Department of Civil Engineering and Hydraulic, Institute of Science and Technology, University Center of Mila. ALGERIA.

⁴University Center of Morsli Abdallah Tipaza. ALGERIA.

⁵Laboratory EOLE, Faculty of Technology, Department of Civil Engineering, Abou Bekr Belkaid University, Tlemcen, Algeria

⁶October High Institute for Engineering and Technology. EGYPT

⁷Faculty of Engineering AL Azhar University. Qena, EGYPT

—^{*1,2} ismahene.civil@yahoo.fr

Abstract

The tunnels are one of the most important constructions that shorten the time and facilitate the transition between difficult places such as highlands and mountains. It is one of the reasons countries grow economically. The tunnels must be safe in all situations. The engineer must take into consideration the quality of the soil and rock in the place of excavation, the appropriate method of excavation, the location of the tunnel, and the materials used, as well as the design of the tunnel without forgetting the appropriate shape of the tunnel. In this paper, we simulated the model with various shapes ("seven shapes") by using the finite element method Optum G2 software. The stability research for the various tunnel shapes was carried out by examining soil settlements, horizontal, vertical displacement, shear, normal forces, and a bending moment of the lining concrete of these shapes.

Keywords: Tunnel, Modelling, FEM, Seven Shapes, Unstable, Optum G2.

1. Introduction

In both urban and rural locations, tunnels and underground spaces are now routinely used for various purposes, including navigating and crossing natural obstacles and enhancing transportation systems (including rail, metro, and other systems). The success of tunnel utilization is also a result of both their resilience and endurance, since they are inherently more resistant to natural disasters like earthquakes, floods, atmospheric, and rockfalls, compared to other infrastructures [1]. The tunnels are

constructed with the ultimate goal of being as short as feasible and overcoming environmental and human constraints that exist in nature.

Conceptually, the tunnelling process may be divided into three parts. Planning (feasibility analysis), which outlines and provides a basic design for the tunnel while identifying the project's constraints and dangers; Second, engineering, which focuses on producing exact, constructible designs; third The pre-construction design of the tunnel and the maintenance plan

will then be created, put into action, and updated [2].

Due to the numerous demanding infrastructure improvements made over the past several years, tunnelling has undergone a lot of technical developments. The purpose of the tunnel, the location, geotechnics, geology, length, diameter, groundwater levels, and the available materials are some of the aspects that affect the methods and technologies used in the tunnelling, without forgetting the shapes of the tunnel. There are several tunnelling construction techniques [3, 4], some of which include:

- Tunnel Boring Machine Method (Slurry TBM, Earth Pressure Balance, Variable Density Tunnel Boring Machine); and
- Cut and Cover Method (Bottom Up; Top Down);
- Jacked Box Method
- Drill and Blast Method (New Austrian Tunnelling Method);

To understand the stability of the tunnel's built-in soil and rock mass, many investigations have been conducted by various researchers and experts [5, 6]. There are many experimental, analytical, and computational approaches that may be used to study the tunnels. Several methods to forecast surface settling brought on by tunnel construction, including the empirical formula method [7-10], elastic strain method [11-14], the airy stress function method [15-19], stochastic medium theory [20-22], centrifuge test method [23,24], and numerical simulation method [25, 26]. Numerous parameters and loading types are typically analyzed for tunnelling using the numerical method [27-31]. They used the finite element method to model the reinforced concrete lining when exposed to impact loading with three stages of rock weathering [32]. With Abaqus software, the FEM has been used to model the tunnel, and they have used the nonlinear elastoplastic material models for the different constitutive

material models, reinforcement, concrete, rock, inside-air of the tunnel, and (TNT). In connection with the blast impact, the behaviour of adjacent rock, as well as weathering, has been researched [33]. With three types of rock, the mountain of Himalayan was analyzed by the FEM, This study is to investigate the effect of varied the overburden pressure and the lining thickness under static blast loading, they also changed the shape of the tunnel (four shapes) [34].

The stability analysis of tunnels with different shapes was studied, they used the finite element method to model different shapes and depths of overburden, under static loading and weathering [35]. Other researchers used Abaqus software to analyze the behaviour of different shapes of tunnels under static and surface blast loading [36]. In most articles, researchers used either two or four shapes and compared them. As for us, in this paper, we will compare seven shapes (Horse-Shoe, circular, Square, Segment, Elliptical, Rectangular, and Egg-shaped), in terms of vertical, horizontal displacements, settlements, deformations, and shear and normal forces with a bending moment of the lining concrete.

2. Numerical Analysis

In this paper, we compared various geometry of tunnels to understand the behavior of these infrastructures and choose the safest one. Seven tunnels with various geometry were modeled using the "OPTUMG2", finite element software. The 2D plane strain analysis with the Mohr-Coulomb criteria represents the elastoplastic model of soil. Figure 1, illustrates the geometry of several tunnel forms (Horse-Shoe, circular, Square, Segment, Elliptical, Rectangular, and Egg-shaped), the concrete lining has a thickness of 0.25 m, and the model has 110 m in width and 52 m in height of the model. The tunnels have

been studied with a diameter of 8 m, the tunnels have a 24-meter overburden depth. The bases of the boundary conditions are fixed see figure 1 (a), and the parameters of the model are shown in Table 1.

The Mohr–coulomb plasticity model has been used to model the soil mass. Table 1 shows the soil and concrete lining modeling features used in our models.

Table 1. Soil and concert lining properties.

Concrete Lining (Symbol)	Value (Unite)
Section area A	2500 (cm ² /m)
Weight W	625 (kg/m/m)
Thickness	25 (cm)
Young's module E	$2.54 * 10^4$ (MPa)
Yield strength	28
Moment of inertia I	$1.302 * 10^5$ (cm ⁴ /m)
Plastic section modules S	$1.563 * 10^4$ (cm ³ /m)
Soil Properties (Symbol)	Value (Unite)
Saturated density γ_{sat}	20.5 (KN/m ³)
Young's module E	43.4 (MPa)
Cohesion c	39.5 (KPa)
Poisson's ratio ν	0.26
Friction angle ϕ	29.5 (°)

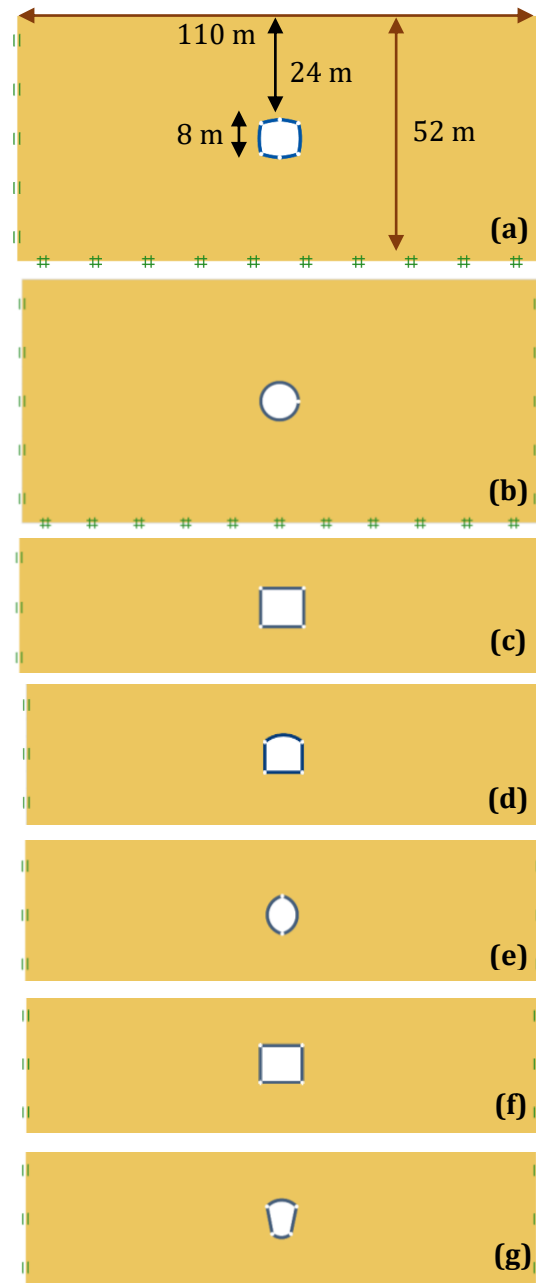


Figure 1. Tunnel Shapes: (a) Horse-Shoe, (b) circular, (c) Square, (d) Segment, (e) Elliptical, (f) Rectangular, (g) Egg-shaped

3. Stages to Modeling the Tunnels

In three stages, the analysis was carried out to imitate real-world conditions:

- a. First Step: During this stage, an initial stress study is performed. It simulates field conditions by having identical soil field characteristics, often known as green field conditions.
- b. Second Step: For the modeling of tunnel excavation, an elastoplastic analysis was done. According to the OPTUM G2 user manual, the tunnel is completely supported, and excavation was completed with full support [37].
- c. The last step: Concrete lining was used to offer support in this stage.

the excavation, the rectangular shape has the maximum settlement with a value of 6.4 cm. We also note the segment and egg-shaped have the same displacements with the value of - 4 cm, and the smallest settlement is -1.5 cm resulting from the elliptical tunnel.

4. Results and Discussion

In this paper, we have modeled all seven shapes in the same way. We assess the displacements vertical and horizontal at the ground surface level ($Y = 52$ m), and near the tunnel at 30.5 m and 21.5 m. Figure 2 shows the Y heights (52 m; 30.5 m; 21.5 m) of the numerical model.

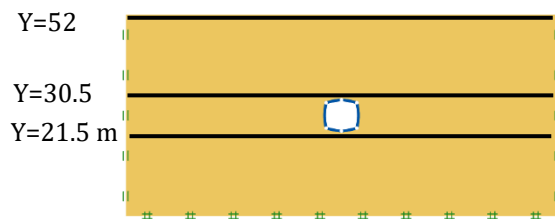


Figure 2. The Y heights of the geometry

4.1 Vertical And Horizontal Displacements

The aim of this study was to carry out the vertical and horizontal displacements using the stated profiles of $Y = 50$, 30.5 m, and 21.5 m. with different numerical shapes of tunnels, figure 3 (a), illustrates the results of settlements and horizontal ($Y = 52$ m) of all shapes. Due to

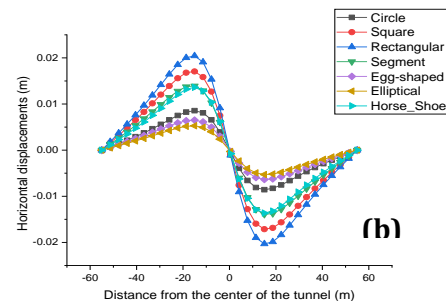
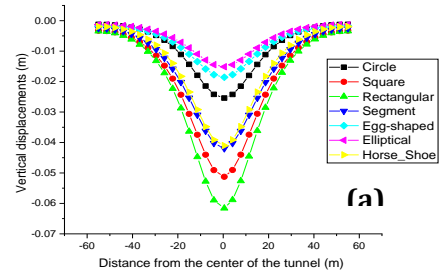


Figure 3. Vertical (a), and Horizontal displacement (b) for $Y = 52$ m

Figure 3 (b) displays the horizontal displacements for various tunnel forms. We note that the horizontal displacements are small compared to the vertical displacement, the maximum horizontal displacement is 2 cm for the rectangular shape, and the minimum displacement is 0.4 cm for the elliptical tunnel. Near the tunnel, at the level of height $Y = 30.5$ m, the maximum settlement is 13.2 cm for the rectangular tunnel as shown in figure 4 (a). The smallest settlement is for the elliptic shape tunnel with a value of 4.2 cm.

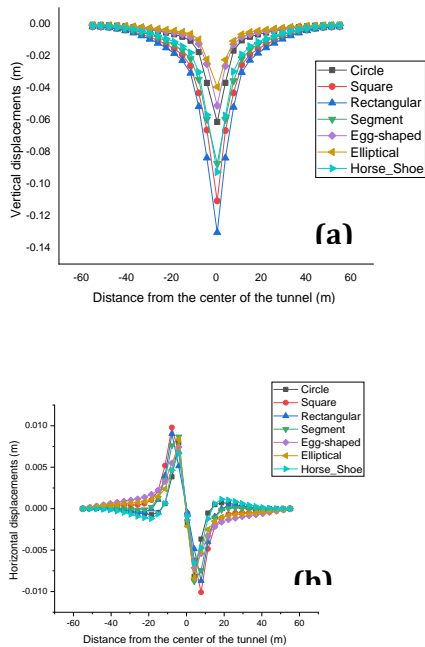


Figure 4. Vertical (a), and Horizontal displacement (b) for $Y = 30.5$ m

Figure 4 (b), clearly shows that at the level of 30.5 m, almost all shapes are of equal horizontal displacement. And the maximum displacement is confined between 10 and 9 cm.

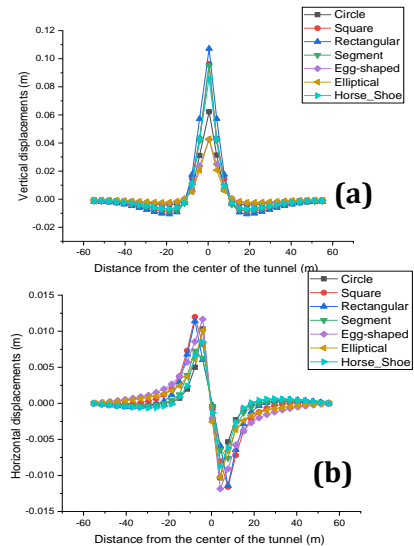


Figure 5. Vertical (a), and Horizontal displacement (b) for $Y = 21.5$ m

At a level of 21.5 m, Figure 5 (a) demonstrates the vertical displacements under the tunnels, we noted a slight settlement (0.5 cm) on the left and right of the tunnels. We have also all vertical displacement going towards the tunnel's center with the maximum displacement is 11 cm from the rectangular tunnel, the smallest displacement is from the elliptical shape (4 cm).

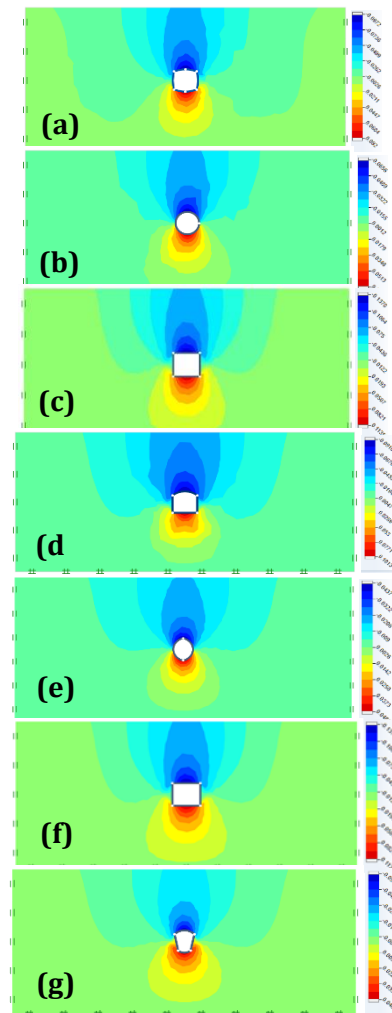


Figure 6. Vertical displacement, (a) Horse-Shoe, (b) circular, (c) Square, (d) Segment, (e) Elliptical, (f) Rectangular, (g) Egg-shaped

At the bottom of the tunnel ($Y=21.5$ m), figure 5 (b), presented the horizontal displacements for all the shapes, there is great consistency in terms of results. And nearly all of the values of the various shapes are the same displacements (1.5 cm).

The vertical displacements are concentrated at the top and bottom of the tunnel as shown in figure 6, this figure illustrated the contour of vertical displacement with seven shapes, and these displacements are symmetrical with regard to the tunnel's vertical axis. The elliptical shape (figure 6 (e)) has a minimum displacement of -0.0437 cm at the top, and 0.0437 at the bottom. After we have the egg-shaped tunnel ± 0.0551 cm (figure 6 (g)).

The horse-Shoe and segment shape have almost the same value (0.09 m). The rectangular shape has the maximum displacements and deformation (± 0.137 m at the peak and at the bottom) of the tunnel as seen in figure 6 (b).

4.2 Bending moment, normal and shear forces of the concrete lining

To more clearly see how the dirt affects the concrete lining. Figures 7, and 8 demonstrate how the displacements and pressure of the soil can result in shear, normal forces, and bending moments around the concrete lining of the tunnel induced by earth movements brought on by excavation. Figure 7, shows the normal forces on the left and right sides of the tunnels, they are the most powerful forces that influence on these types of tunnels. The smallest normal force from elliptical shape (figure 7 (e)), with the value of -507.02 kN. The rectangular shape has a maximum normal force of -697.36 kN. The same shape of the tunnel (rectangular) has the biggest shear forces with the value of -

589.91 kN (figure 7 (f)). Whereas, figure 7 (b), illustrates that the circular shape has the smallest shear force of -19.525 kN.

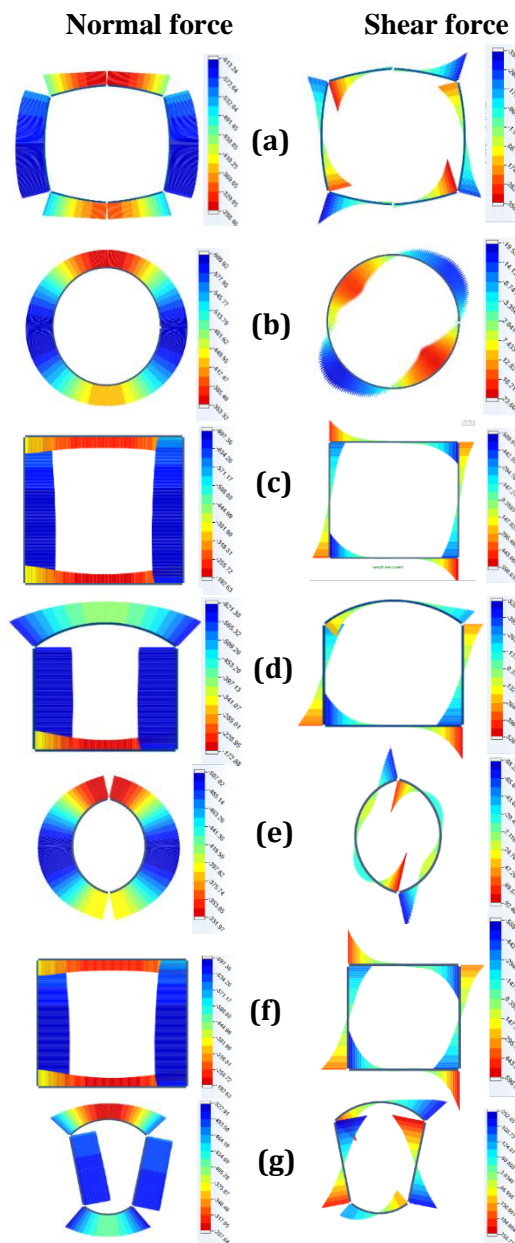


Figure 7. Normal and Shear forces, (a) Horse-Shoe, (b) circular, (c) Square, (d) Segment, (e) Elliptical, (f) Rectangular, (g) Egg-shaped

Finally, as shown in figure 8, the distribution bending moment is symmetrical with respect to the tunnel's vertical axis because of the pressure of the earth around it. This figure (8), illustrates the bending moments of these shapes of tunnels. The circular one has the smallest bending moment (figure 8 (b)) with a value of -34.897 KN.m, whereas the rectangular shape has the biggest value of - 437.466 KN.m, as shown in figure 8 (f). The elliptical tunnel has a value of - 41.10 kN.m he is also small bending moment (figure 8 (e)). And there are minor differences between the two shapes the segment and horseshoe tunnels figure 8 (d) and (a).

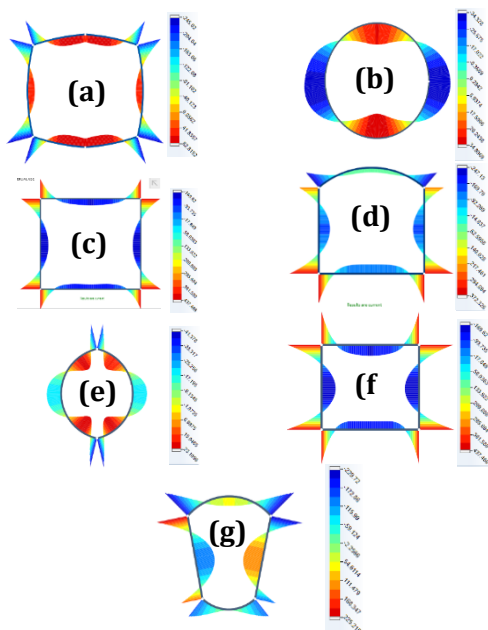


Figure 8. Bending Moment, (a) Horse-Shoe, (b) circular, (c) Square, (d) Segment, (e) Elliptical, (f) Rectangular, (g) Egg-shaped

5. Conclusion

To understand how the shifting shapes behave in stable tunnels. In this study, the two-dimensional finite element method has been used by the OptumG2 software. We assess the model's displacements,

settlements, shear, normal pressures, and bending moment. The outcomes amply demonstrate that the safe one is the elliptical tunnel due to their numerical analysis results, because having the smallest vertical and horizontal displacements, the minimum normal force, and the lowest bending moment among these seven shapes. We have also the circular tunnel takes second place in safety after the elliptical tunnel, the circular shape has the smallest shear force, and the values of the bending moment and normal force are near to the values of the elliptical tunnel. The unstable tunnel between the seven shapes is the rectangular, results explain this decision. The maximum displacements vertical and horizontal, the biggest normal, shear forces between these shapes. All these results are related to the rectangular shape of the tunnel.

References

- [1] C. di Prisco, D. Peila, A. Pigorini. "Handbook on Tunnels and Underground Works" Chapter "Introduction". 1st Edition, 2022, CRC Press, ISBN 9781003256175.
- [2] C. di Prisco, L. Flessati, D. Peila, E.M. Pizzarotti. Book "Handbook on Tunnels and Underground Works" Chapter "Risk management in tunnelling". 1st Edition, 2022, CRC Press, ISBN 9781003256175.
- [3] M. Faraz Athar, Mohammad Zaid, Md. Rehan Sadique, (2019) "Stability of Different shapes of Tunnels in Weathering Stages of Basalt", In Proceedings: National Conference on Advances in Structural Technologies (CoAST-2019), NIT Silchar, Silchar, India.
- [4] Zainul Abedin Khana, Md Shahab Khana, M. R. Sadiquea, Manojit Samantab, Mohd. Masroor . Alama Response of Twin Transportation Tunnel in Earthquake Loading: A

Review. 2021 IOP Conf. Ser.: Earth Environ. Sci. 796012044.

[5] Carranza-Torres C, Fairhurst C (1999) The elasto-plastic response of underground excavations in rock masses that satisfy the Hoek-Brown failure criterion. *Int J Rock Mech Min Sci* 36:777–809. [https://doi.org/10.1016/S01489062\(99\)00047-9](https://doi.org/10.1016/S01489062(99)00047-9)

[6] Ouchi A, Pakalnis R, AGM-CIM TB (2004) Update of span design curve for weak rock masses. In: Proceedings of the 99th annual AGM-CIM conference. Edmonton, AB

[7] R. B. Peck, “Deep excavations and tunnelling in soft ground,” in Proceedings of the Seventh International Conference on Soil Mechanics and Foundation Engineering, pp. 225–290, Mexico City, Mexico, August 1969.

[8] P. B. Attewell and J. P. Woodman, “Predicting the dynamics of ground settlement and its derivatives caused by tunneling in soil,” *International Journal of Rock Mechanics and Mining Sciences & Geomechanics Abstracts*, vol. 15, no. 8, pp. 13–22, 1982

[9] R. J. Mair, R. N. Taylor, and A. Bracegirdle, “Subsurface settlement profiles above tunnels in clays,” *Géotechnique*, vol. 45, no. 2, pp. 361–362, 1995.

[10] M. Lei, J. Liu, Y. Lin, C. Shi, and C. Liu, “Deformation characteristics and influence factors of a shallow tunnel excavated in soft clay with high plasticity,” *Advances in Civil Engineering*, vol. 2019, Article ID 7483628, 14 pages, 2019.

[11] C. Sagaseta, “Analysis of undrained soil deformation due to ground loss,” *Géotechnique*, vol. 37, no. 3, pp. 301–320, 1987.

[12] A. Verruijt and J. R. Booker, “Surface settlements due to deformation of a tunnel in an elastic half plane,” *Géotechnique*, vol. 46, no. 4, pp. 753–756, 1996.

[13] N. Loganathan and H. G. Poulos, “Analytical prediction for tunneling-induced ground movements in clays,” *Journal of Geotechnical and Geoenvironmental Engineering*, vol. 124, no. 9, pp. 846–856, 1998.

[14] B. Zeng, D. Huang, and J. He, “Analysis of double-O-tube shield tunnelling-induced soil deformation due to ground loss,” *Géotechnique Letters*, vol. 6, no. 1, pp. 7–15, 2016.

[15] A. M. M. Wood, “the circular tunnel in elastic ground,” *Géotechnique*, vol. 25, no. 1, pp. 115–127, 1975.

[16] A. Bobet, “Analytical solutions for shallow tunnels in saturated ground,” *Journal of Engineering Mechanics*, vol. 127, no. 12, pp. 1258–1266, 2001.

[17] K. H. Park, “Elastic solution for tunneling-induced ground movements in clays,” *International Journal of Geomechanics*, vol. 4, no. 4, pp. 310–318, 2004.

[18] K.-H. Park, “Analytical solution for tunnelling-induced ground movement in clays,” *Tunnelling and Underground Space Technology*, vol. 20, no. 3, pp. 249–261, 2005.

[19] A.M.Puzrin, J.B.Burland, and J.R.Standing, “Simple approach to predicting ground displacements caused by tunnelling in undrained anisotropic elastic soil,” *Géotechnique*, vol. 62, no. 4, pp. 341–352, 2012.

[20] J. Litwiniszyn, “The theories and model research of movements of ground masses,” in Proceedings of the European Congress Ground Movement, pp. 203–209, Leeds, UK, April 1957.

[21] K. Wu, Z. S. Shao, S. Qin, and B. X. Li, “Determination of deformation mechanism and countermeasures in silty clay tunnel,” *Journal of Performance of Constructed Facilities*, 2019.

[22] X. L. Yang and J. M. Wang, “Ground movement prediction for tunnels using

simplified procedure,” *Tunnelling and Underground space Technology*, vol.26, no.3, pp. 462–471,2011.

[23] D.J. White, W.A. Take, and M.D. Bolton, “Soil deformation measurement using particle image velocimetry (PIV) and photogrammetry,” *Géotechnique*, vol. 53, no. 7, pp. 619–631,2003.

[24] G. Song and J. A. Black, “Soil Displacement due to tunnelling using small-scale centrifuge technology,” in *Proceedings of the 3rd European Conference on Physical Modelling in Geotechnics (ECPMG 2016)*, Nantes, France, June 2016.

[25] Y. Cheng, Z. Song, J. Jin, and T. Yang, “Attenuation characteristics of stress wave peak in sandstone subjected to different axial stresses,” *Advances in Materials Science and Engineering*, vol. 2019, Article ID 6320601, 11 pages, 2019.

[26] G. Swoboda and A. Abu-Krishna, “Three-dimensional numerical modelling for TBM tunnelling in consolidated clay,” *Tunnelling and Underground Space Technology*, vol.14, no. 3, pp. 327–333, 1999.

[27] Irfan Ahmad Shah, and Mohammad Zaid. Behavior of Underground Tunnel under Strong Ground Motion. *Proceedings of Indian Geotechnical Conference 2020*. December 17-19, 2020, Andhra University, Visakhapatnam.

[28] Zaid, M., Irfan, S., Farooqi, M.A. (2019). Effect of Cover Depth in Unlined Himalayan Tunnel: A Finite Element Approach. In the proceeding of 8th Indian Rock Conference, Indian International Centre, New Delhi, India, 03-04 March 2019, ISBN No. 81-86501-27-1.

[29] Shahin, H. M., Nakai, T., Zhang, F., Kikumoto, M., & Nakahara, E. (2011). Behavior of ground and response of existing foundation due to tunneling. *Soils and foundations*, 51(3), pp. 395-409.

[30] Pakbaz, M. C., & Yareevand, A. (2005). 2-D analysis of circular tunnel against earthquake loading. *Tunnelling and Underground Space Technology*, 20(5), 411-417.

[31] Mroueh, H., & Shahrour, I. (2003). A full 3-D finite element analysis of tunneling adjacent structures interaction. *Computers and Geotechnics*, 30(3), 245-253.

[32] Zaid, M. Preliminary Study to Understand the Effect of Impact Loading and Rock Weathering in Tunnel Constructed in Quartzite. *Geotech Geol Eng* (2021). <https://doi.org/10.1007/s10706-021-01948-z>.

[33] Zaid, M., Sadique, M.R. & Alam, M.M. Blast Resistant Analysis of Rock Tunnel Using Abaqus: Effect of Weathering. *Geotech Geol Eng* 40, 809–832 (2022). <https://doi.org/10.1007/s10706-021-01927-4>

[34] Zaid, M., Shah, I.A. Numerical Analysis of Himalayan Rock Tunnels under Static and Blast Loading. *Geotech Geol Eng* 39, 5063–5083 (2021). <https://doi.org/10.1007/s10706-021-01813-z>

[35] Mohd. Faraz Athar, Mohammad Zaid, Md. Rehan Sadique. (2019) Stability of Different shapes of Tunnels in Weathering Stages of Basalt. *Proceedings of National Conference on Advances in Structural Technologies (CoAST-2019)*, 1-3 Feb, 2019 Department of Civil Engineering National Institute of Technology Silchar.

[36] Mohammad Zaid. Irfan Ahmad Shah (2021). Numerical Analysis of Himalayan Rock Tunnels under Static and Blast Loading. *Geotech Geol Eng* (2021) 39:5063–5083. [https://doi.org/10.1007/s10706-021-01813-z\(0123456789\(\).,-volV\)](https://doi.org/10.1007/s10706-021-01813-z(0123456789().,-volV)).

[37] Krabbenhoft, K., Lyamin, A., & Krabbenhoft, J. (2015). Optum computational engineering (OptumG2). Computer software]. Retrieved from <https://www.optumce.com>.